


 Cite this: *RSC Adv.*, 2025, 15, 42176

# Enhancement of antimicrobial and structural properties of PVA packaging films using neem leaf powder: an example for extending the shelf life of cowpeas

 TamilAnand Solaikannan,<sup>id</sup><sup>a</sup> Sivaranjana Paramasivan,<sup>\*a</sup> Rajini Nagarajan<sup>b</sup> and Nadir Ayrilmis<sup>id</sup><sup>\*c</sup>

This study focused on the fabrication and characterization of polyvinyl alcohol (PVA)/*Azadirachta indica* (neem leaf) hybrid films for use in active food packaging. PVA/AiP hybrid films were prepared using a solution casting technique with varying concentrations of AiP (0.1, 0.5, 1.0, 1.5, and 2.0 g) as a bio-filler. The films were comprehensively characterized using FTIR, XRD, SEM, optical microscopy, TGA/DSC, water absorption, oxygen permeability, mechanical strength, water vapor transmission rate, soil degradability, and antimicrobial activity tests. TGA/DSC showed improved thermal stability of the hybrid films (up to 330 °C) with increasing AiP content. Water absorption increased with AiP incorporation, peaking at 0.5 g, (130% at 60 min) while oxygen permeability was highest for the 0.5 g AiP film (~8.0 mg L<sup>-1</sup> at 72 hours). At 2 g AiP loading, the film showed noticeable brittleness, making it unsuitable for conventional film applications. Hence, it was not compared with the lower concentration films, but its barrier properties were evaluated separately. Tensile strength significantly improved at 2 g AiP loading (18.82 MPa). Water vapor transmission rate progressively reduced with increasing AiP content. Soil degradability was enhanced at 0.1 g AiP (74.5%) but decreased at higher loadings (55.4%). Antimicrobial activity against *E. coli* increased with AiP concentration. Compared to pure PVA films (tensile strength 12–15 MPa, WVTR 6.0–7.2 g mm m<sup>-2</sup> day<sup>-1</sup> kPa<sup>-1</sup>) and commercial PET films (tensile strength 55–75 MPa, WVTR 2.0–3.0 g mm m<sup>-2</sup> day<sup>-1</sup> kPa<sup>-1</sup>), the PVA/AiP hybrid films exhibited superior barrier performance and antimicrobial activity while being biodegradable. The findings demonstrated the potential of PVA/AiP hybrid films as sustainable and effective active food packaging materials. This supports the achievement of sustainable development goal (SDG) 12, which focuses on responsible consumption and production. Unlike pure PVA or conventional plastics, PVA/AiP hybrid films combined superior performance with biodegradability and antimicrobial activity.

 Received 29th July 2025  
 Accepted 17th October 2025

DOI: 10.1039/d5ra05486a

[rsc.li/rsc-advances](http://rsc.li/rsc-advances)

## 1 Introduction

The environmental problems caused by plastic packaging have raised concerns worldwide. This has increased the demand for sustainable and biodegradable materials for the food industry. The move toward sustainable packaging is driven not only by environmental concerns but also by changing consumer preferences for eco-friendly products.<sup>1,2</sup> People now prefer

packaging, which reduces harm to the environment and supports responsible use of resources. Developing and using sustainable food packaging is essential to reduce the negative effects of plastics and to support a more environmentally friendly food system. Active packaging is becoming increasingly popular as a way to reduce food waste and improve food quality. It contains active ingredients that help extend shelf life and keep food safer.<sup>3,4</sup> This approach offers a smart solution to meet consumer demand and sustainability goals in food packaging. Unlike passive packaging, which primarily serves as a barrier against external factors, active packaging interacts directly with food products or the surrounding environment to inhibit microbial growth, scavenge oxygen, absorb moisture, or release antimicrobial agents.<sup>5</sup> This proactive approach helps maintain food freshness, prevent spoilage, and minimize the risk of foodborne illnesses, ultimately extending the shelf life of perishable goods and reducing the amount of food that ends up

<sup>a</sup>Department of Chemistry, School of Advanced Sciences, Kalasalingam Academy of Research and Education, Krishnankoil-626126, Tamilnadu, India. E-mail: [psivaranjana@gmail.com](mailto:psivaranjana@gmail.com)

<sup>b</sup>Department of Mechanical Engineering, School of Mechanical, Automobile, Aeronautical and Civil Engineering, Kalasalingam Academy of Research and Education, Krishnankoil, Tamilnadu-626126, India

<sup>c</sup>Department of Wood Mechanics and Technology, Faculty of Forestry, Istanbul University-Cerrahpasa, Bahcekoy, Sariyer, 34473 Istanbul, Turkey. E-mail: [nadiray@istanbul.edu.tr](mailto:nadiray@istanbul.edu.tr)



in landfills. The use of biodegradable polymers and natural additives is key to creating eco-friendly food packaging. These materials help reduce the use of traditional plastics and environmental pollution. They offer a sustainable solution that supports both food safety and environmental protection.<sup>6</sup> Polyvinyl alcohol (PVA) is a biocompatible and biodegradable synthetic polymer that has been widely used in various packaging applications owing to its excellent film-forming properties, water solubility, and nontoxic nature.<sup>7</sup> PVA has some limitations, such as being water-loving (hydrophilic), lacking natural antibacterial properties, and weak mechanical and thermal strength. Therefore, they often need to be combined with other materials to improve their performance. The addition of reinforcements and active agents makes PVA more suitable for food packaging applications.<sup>8</sup>

*Azadirachta indica* (neem) leaf extract is a well-known natural product that possesses potent antimicrobial properties, making it a suitable active ingredient for incorporation into food packaging films to inhibit microbial growth and extend the shelf life of perishable goods.<sup>9,10</sup> Neem leaves contain a complex mixture of bioactive compounds, including azadirachtin, nimbin, and nimbidin,<sup>11</sup> which exhibit broad-spectrum antimicrobial activities against bacteria, fungi, and viruses. Combining PVA with *Azadirachta indica* leaf powder (AiP) can potentially create a hybrid film with enhanced mechanical properties and antimicrobial activity, thereby offering a promising approach for developing sustainable and effective active food packaging solutions.<sup>12</sup> The implementation of PVA/AiP hybrid films can support the achievement of SDG targets related to waste reduction, sustainable consumption, and responsible production in the food industry by providing a sustainable and effective alternative to conventional plastic packaging.<sup>13,14</sup>

Recent studies have explored the incorporation of various plant-derived extracts into PVA matrices to develop bioactive packaging films with antimicrobial and antioxidant functions. For instance, PVA films containing green tea extract have shown improved barrier properties, pH sensitivity, and strong antioxidant activity.<sup>15</sup> Similarly, the integration of basil leaf extract with cellulose nanocrystals in PVA films enhanced tensile strength and imparted notable antimicrobial and antioxidant effects.<sup>16</sup> Neem extract has also been successfully incorporated into PVA–chitosan nanofibrous mats, demonstrating broad-spectrum antibacterial activity and improved thermal stability.<sup>17</sup> Other plant-derived actives such as eugenol-rich essential oils,<sup>18</sup> curcumin,<sup>19</sup> and black tea polyphenols<sup>20</sup> have likewise been embedded into PVA-based films, contributing to active food packaging by retarding spoilage and extending shelf life. While these studies highlight the versatility of PVA as a carrier for bioactive compounds, most reported systems rely on extracts, oils, or purified derivatives, often requiring additional processing steps.

In contrast, the novelty of this work lies in the direct utilization of neem leaf powder (AiP) without any chemical processing or hazardous treatments as a functional filler in PVA films. This green approach shows that neem leaf powder can effectively impart multifunctional benefits, including antimicrobial activity, improved barrier performance, biodegradability and balanced mechanical strength, even in its natural,

unprocessed form. These benefits are imparted to the hybrid films. Active food packaging materials require a combination of key properties, including mechanical strength, barrier performance (oxygen and moisture), thermal stability, biodegradability, and antimicrobial activity. The PVA/AiP hybrid films developed in this study provide a balanced combination of these features, demonstrating their potential as effective and sustainable packaging solutions. At the same time, it valorizes neem leaf biomass, which is abundantly available as agricultural waste in India, thereby contributing to circular economy principles. This article highlights biodegradable materials as a sustainable alternative to conventional plastics, helping address environmental issues and support SDG 12<sup>21</sup> (responsible consumption and production) by reducing waste and greenhouse gas emissions.

This study aimed to fabricate and characterize PVA/AiP hybrid films, comprehensively evaluating their physical, mechanical, and antimicrobial properties to assess their suitability for active food packaging applications, with a focus on optimizing film composition and performance. The fabrication process involved combining PVA with varying concentrations of AiP using a solution casting technique, followed by thorough characterization using a range of analytical methods such as X-ray diffraction (XRD), Scanning electron microscopy (SEM), Fourier-transform infrared spectroscopy (FTIR), Thermogravimetric analysis (TGA), and Differential Scanning Calorimetry (DSC). Physical properties such as water absorption, oxygen permeability, water vapor transmittance rate, and biodegradability were measured to assess the integrity and barrier properties of the film. Mechanical properties such as the tensile strength, elongation at break, and Young's modulus were evaluated to determine the ability of the film to withstand stress and maintain its structural integrity. The developed PVA/AiP hybrid films not only outperform pure PVA but also show competitive strength and barrier properties compared to other reported bio-based films, while offering biodegradability and antimicrobial activity absent in commercial plastics such as PE (polyethylene) and PP (polypropylene). This balanced performance highlights their novelty and potential as sustainable alternatives for active food packaging.

## 2 Materials and methods

### 2.1 Materials

Polyvinyl alcohol (PVA) with a molecular weight of 86.19 g mol<sup>-1</sup>, was purchased from GS Scientific Chemicals, Madurai, Tamil Nadu, India. *Azadirachta indica* leaves were sourced from the KARE Campus in Krishnankoil, Tamil Nadu, India. Dimethyl sulfoxide (DMSO) was obtained from GS Scientific Chemicals (Madurai, Tamil Nadu, India). All the chemicals and reagents used in this study were of analytical grade.

### 2.2 Methods

**2.2.1 Fabrication of PVA/AiP hybrid films.** Fresh *Azadirachta indica* (neem) leaves were collected, thoroughly washed with distilled water, and dried in a hot-air oven at 40 °C for 24 h. The dried leaves were finely powdered using a grinder, and the



resulting powder was sieved to obtain a uniform particle size. The final neem leaf powder fraction collected corresponded to particles in the range of 250–600  $\mu\text{m}$  which was used for film preparation. Separately, 1 g of polyvinyl alcohol (PVA) was dissolved in 10 mL of dimethyl sulfoxide (DMSO) to prepare a 10% (w/v) PVA solution. The mixture was continuously stirred at 60 °C for 1 h until a clear solution was obtained. To fabricate the hybrid films, the solution casting technique was employed using PVA as the matrix and *Azadirachta indica* powder (AiP) as the bio-filler. The AiP was first dispersed in the solvent and sonicated for a few minutes to ensure uniform dispersion, followed by thorough stirring of the PVA solution. The films were dried under normal ambient conditions at room temperature for 6 days, after which they were gently peeled from the casting surface. Hybrid films were prepared using varying concentrations of AiP (0.1 g, 0.5 g, 1.0 g, 1.5 g, and 2.0 g). The fabrication process of the PVA/AiP hybrid films is presented in Fig. 1.

Thickness of the PVA/AiP hybrid films was measured using a Make-Tesa Microhite 3D, and the average thickness was measured. The thickness of the films was added in Table 1.

All experiments were performed in triplicate to ensure reproducibility of the results. The mean values were calculated, and the standard deviation (SD) of the measurements was used to represent variability in the data. These SD values were used to construct error bars in the figures.

Table 1 Thickness of the matrix PVA film and PVA/AiP hybrid films

Sample	Thickness (mm)
PVA	0.204
PVA/AiP with 0.1 g of AiP	0.207
PVA/AiP with 0.5 g of AiP	0.218
PVA/AiP with 1 g of AiP	0.202
PVA/AiP with 1.5 g of AiP	0.211
PVA/AiP with 2 g of AiP	0.555

**2.2.2 Fourier transform infrared spectroscopy (FTIR) analysis.** The FTIR was used to investigate the chemical interactions between polyvinyl alcohol (PVA) and *Azadirachta indica* powder (AiP) in the hybrid films. Analysis was performed using a Shimadzu IR Tracer-100 spectrometer. Spectra were recorded in the range of 4000  $\text{cm}^{-1}$  to 400  $\text{cm}^{-1}$ , with 45 scans performed at a resolution of 0.2  $\text{cm}^{-1}$  for each sample, ensuring accurate identification of functional groups and potential interactions between the polymer matrix and the bio-filler.

**2.2.3 X-ray diffraction (XRD).** The crystallinity of the PVA/AiP hybrid films was evaluated using XRD. Diffraction patterns were recorded using a Bruker D8 Advance ECO (A25) XRD system equipped with an SSD160 1D detector. The instrument was operated with Cu K $\alpha$  radiation ( $\lambda = 1.541 \text{ \AA}$ ) at a voltage of 40 kV and current of 35 mA. Scans were conducted

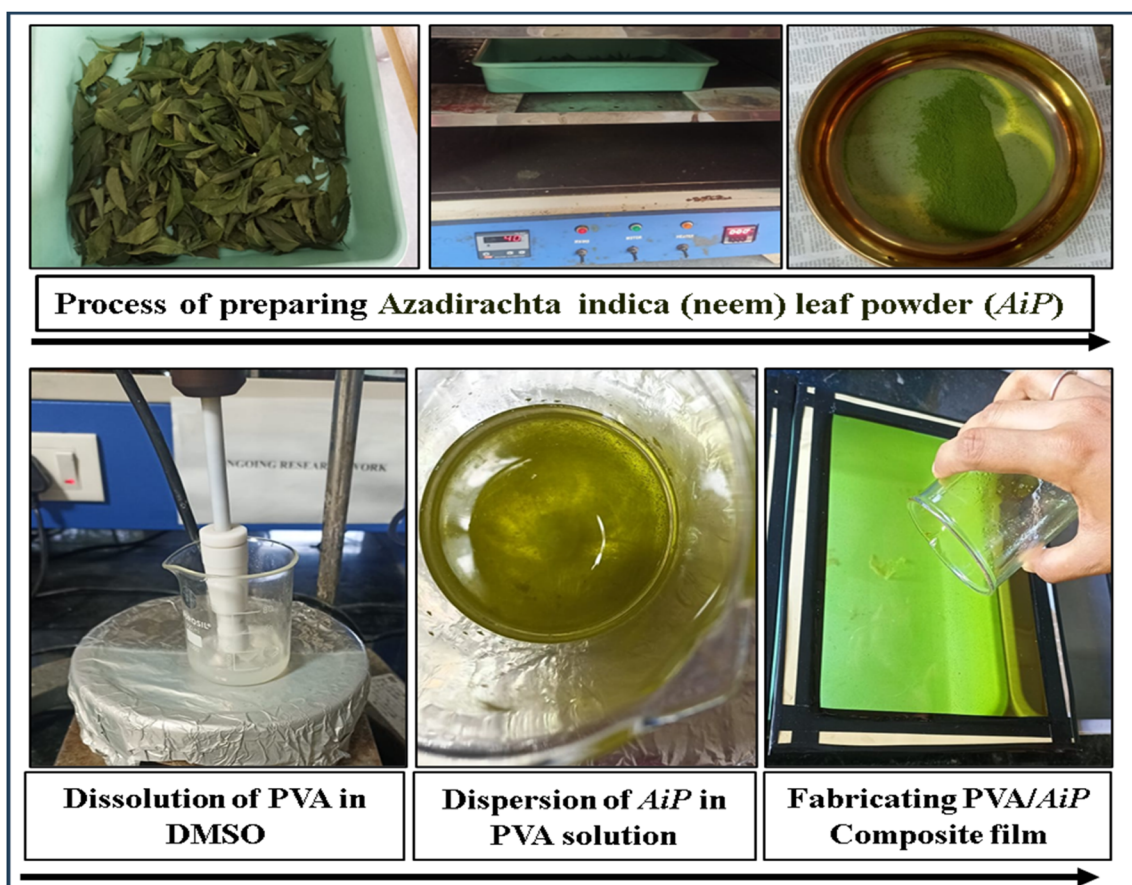


Fig. 1 The fabrication process of the PVA/AiP hybrid films.



over a  $2\theta$  range of 10–80°, with a step size of 0.020° per scan. This analysis provides insights into the crystalline structure and phase distribution of the hybrid films.

**2.2.4 Morphological analysis.** The surface morphologies of the PVA/AiP hybrid films were examined using Scanning electron microscopy (SEM) (Carl Zeiss EVO 18). The analysis was performed at an accelerating voltage of 20 kV to acquire secondary electron (topographic) images. Prior to imaging, the film samples were sputter-coated with a thin (~20 nm) layer of gold–palladium (Au–Pd) using a high-resolution sputter coater to enhance conductivity and image clarity. The SEM images provided detailed insights into the dispersion of AiP within the PVA matrix and the overall surface texture of the hybrid films.

The dispersion of *Azadirachta indica* powder (AiP) within the PVA matrix of the hybrid films was analyzed using an optical microscope (Motic MLC-150c, Moticam 2500). The system is equipped with a 1/3-inch sensor and offers a resolution of 2592 × 1944 pixels, with a pixel pitch of 2.2 μm × 2.2 μm. The microscope features a USB 2.0 interface for data transfer and is powered *via* USB. This analysis allowed for visual assessment of the filler distribution and uniformity within the hybrid films.

**2.2.5 Thermogravimetric and differential scanning calorimetry (TGA/DSC) analysis.** The thermal stability and transitions of the PVA/AiP hybrid films were investigated using Thermogravimetric Analysis (TGA) and Differential Scanning Calorimetry (DSC) performed on a PerkinElmer STA 8000 system. TGA was conducted under nitrogen atmosphere at a flow rate of 20 mL min<sup>-1</sup> using approximately 5 mg of the sample. The temperature was ramped from 20 to 700 °C at a heating rate of 10 °C min<sup>-1</sup>, and the thermal degradation behavior was assessed based on the weight loss and residual mass at 700 °C. DSC analysis was performed under a nitrogen flow of 50 mL min<sup>-1</sup> using approximately 5 mg of the sample sealed in an aluminum pan, with an empty pan as a reference. The temperature range for DSC was set from -50 °C to 300 °C at a heating rate of 10 °C min<sup>-1</sup>. Thermograms were analyzed to determine the glass transition temperature ( $T_g$ ), melting temperature ( $T_m$ ), and associated enthalpy changes ( $\Delta H$ ), providing insights into the thermal transitions of the hybrid films.

**2.2.6 Water absorption test.** The water absorption behavior of the PVA/AiP hybrid films was evaluated by measuring the amount of water absorbed over a fixed period. Uniformly sized film samples (1 × 1 cm<sup>2</sup>) were prepared, and their initial dry weights ( $m_d$ ) were recorded.<sup>22</sup> Subsequently, the films were immersed in distilled water for 2 h. After immersion, the films were gently blotted with tissue paper to remove surface moisture and reweighed to obtain the wet weight ( $m_w$ ).<sup>23</sup> The percentage of absorbed water was calculated using the eqn (1):

$$\text{Water absorption (\%)} = \left( \frac{m_w - m_d}{m_d} \right) \times 100 \quad (1)$$

The swelling behavior of hybrid films is influenced by several factors, including the crosslinking density, film morphology, composition, and the presence of fillers such as AiP. These parameters collectively affect the performance of the film and

its ability to absorb and retain moisture, which is critical for various packaging and biomedical applications.<sup>24</sup>

**2.2.7 Oxygen permeability test.** Oxygen permeability of the PVA/AiP hybrid films was assessed using a flask-based method. Each film specimen was carefully sealed over the opening of a 250 mL flask containing 200 mL of deionized water. Prior to sealing, the initial dissolved oxygen (DO) level of the water was measured using a calibrated DO meter (Lutron). Only samples with comparable initial DO values (within ±0.2 mg L<sup>-1</sup>) were used to ensure standardization across tests.<sup>25</sup>

The sealed flasks were then exposed to ambient air under constant agitation for 24 h to simulate permeation conditions. A tightly sealed flask (zero oxygen ingress) was used as the negative control, and an unsealed flask was used as the positive control. After the test period, final DO values were recorded. The difference between the initial and final DO levels was used to estimate oxygen permeability, providing a comparative measure of the barrier performance of the films. The change in DO levels before and after the test period indicates the oxygen permeability of the films, providing insight into their potential as barrier materials in packaging applications.<sup>26,27</sup>

**2.2.8 Mechanical properties.** The mechanical strength of the PVA/*Azadirachta indica* powder (AiP) hybrid films was measured using a tensile testing machine (WDW-10E, TE China, Microlab Testing Private Limited, Ambattur Industrial Estate, Chennai). The films, with dimensions of 150 mm length and 15 mm breadth, were tested under a load using a 1-ton capacity machine. Five samples from each category were tested, and the average tensile strength was reported. This analysis provided valuable information about the tensile properties, including the elongation at break and ultimate tensile strength, which are critical for evaluating the suitability of films for various applications in packaging.

**2.2.9 Water vapour transmission rate.** WVTR was determined using a gravimetric method under controlled conditions, the rate at which water vapor permeates a PVA/AiP hybrid films is measured by its water vapour transmission rate (WVTR). 10 mL of deionized water was placed in bottles with mouth diameters of 2 cm ( $A$ ) in order to test the WVTR. Teflon tape was used to firmly seal the mouths of the bottles after the polymer films were placed over them to guarantee an airtight closure. After determining the initial weight ( $w_i$ ) of each bottle, the bottles were placed in an oven at 40 °C for 24 h ( $t$ ). The bottles were removed from the oven and weighed again after the incubation period ( $w_f$ ). The eqn (2) was used to obtain the water vapor transfer rate (WVTR).<sup>28</sup>

$$\text{WVTR} = \frac{w_i - w_f}{A \times t} \quad (2)$$

A lower water vapor transmission rate (WVTR) denotes improved barrier qualities, indicating that the film is more successful in stopping water vapor from spreading. This feature is particularly advantageous in applications such as food packaging, where moisture protection is essential.<sup>29</sup>

**2.2.10 Soil degradability.** After weighing, the PVA and PVA/AiP films (2 × 2 cm) were buried in compost soil 5 cm below the



surface. The samples were cultured at room temperature for six weeks. Every day, approximately 2 mL of water was supplied to the samples to maintain moisture levels and encourage microbial activity. The final weights of the film samples were noted after a six-week incubation period. While the PVA films served as sources of carbon for microorganisms, the addition of water promoted microbial activity in the compost. This eqn (3) was used to determine the weight loss of the samples, which is an indication of biodegradation.

$$\text{Weight loss (\%)} = \frac{(w_i - w_d)}{w_i} \times 100 \quad (3)$$

where  $W_i$  is the initial weight of the PVA and PVA/AiP films and  $W_d$  is the dried weight of the PVA and PVA/AiP films.

**2.2.11 Test for antibacterial activity (disk diffusion method).** The disk diffusion method was employed to assess the antibacterial activity of the PVA and PVA/AiP hybrid films with varying concentrations. The antibacterial activity of the prepared films was evaluated against *Escherichia coli* (ATCC 25922), a representative Gram-negative bacterium. The bacterial culture was standardized to 0.5 McFarland standard ( $\approx 1 \times 10^8$  CFU mL<sup>-1</sup>) prior to use. The agar well diffusion method was employed, in which film samples were placed on Mueller–Hinton agar plates inoculated with the standardized bacterial suspension. The plates were incubated at 37 °C for 24 h under aerobic conditions. After incubation, the inhibition zones around the films were measured. Mueller–Hinton agar plates were prepared by inoculating them with bacterial suspensions, placing PVA and PVA/AiP hybrid films (4 cm<sup>2</sup>) on the agar surface, incubating the plates, and measuring the area of inhibition. Positive and negative controls were included to validate the results, and all procedures were conducted aseptically. The susceptibility or resistance of the tested bacteria was

determined by comparing the area of inhibition to standard interpretive charts, allowing for the evaluation of the antibacterial properties of the PVA and PVA/AiP hybrid films with varying concentrations.

**2.2.12 Application of films for food packaging.** The produced PVA/AiP films were tested as active packaging for fresh cowpeas in order to assess their practical usability. To ensure full surface coverage, the films were wrapped around 5 g of freshly taken cowpeas. Cowpeas that had not been wrapped served as the control. Every sample was kept in standard laboratory settings, which included  $28 \pm 2$  °C and 60–70% relative humidity. Periodically, the cowpeas were checked for microbiological spoiling, texture and visual appearance (color changes, fungal growth, and shrinking). The shelf life of the wrapped samples and the unwrapped controls were compared when the storage duration was extended until obvious indications of spoiling were seen.

## 3 Results and discussion

### 3.1 FTIR spectral analysis

To explore the type of interaction between the PVA matrix and AiP filler, the FTIR spectrum of the PVA matrix (Fig. 2a), and PVA/AiP hybrid films (Fig. 2b) at different concentrations is shown in (Fig. 2b). The FTIR spectrum of the PVA matrix revealed a broad peak at 3276 cm<sup>-1</sup>, indicating –OH stretching due to hydrogen bonding, 2905 cm<sup>-1</sup> corresponding to –CH<sub>2</sub> stretching, the peak at 1712 cm<sup>-1</sup> suggesting the existence of a carbonyl group, 1613 cm<sup>-1</sup> for H–O–H bending (water absorption), highlighting PVA's hydrophilic nature of PVA, 1432 cm<sup>-1</sup> for C–H bending, and 1292 cm<sup>-1</sup> for –CH (wagging). The PVA backbone was marked by a C–O stretching peak for alcohol at 1054 cm<sup>-1</sup> and a C–C stretching peak at 824 cm<sup>-1</sup>. In

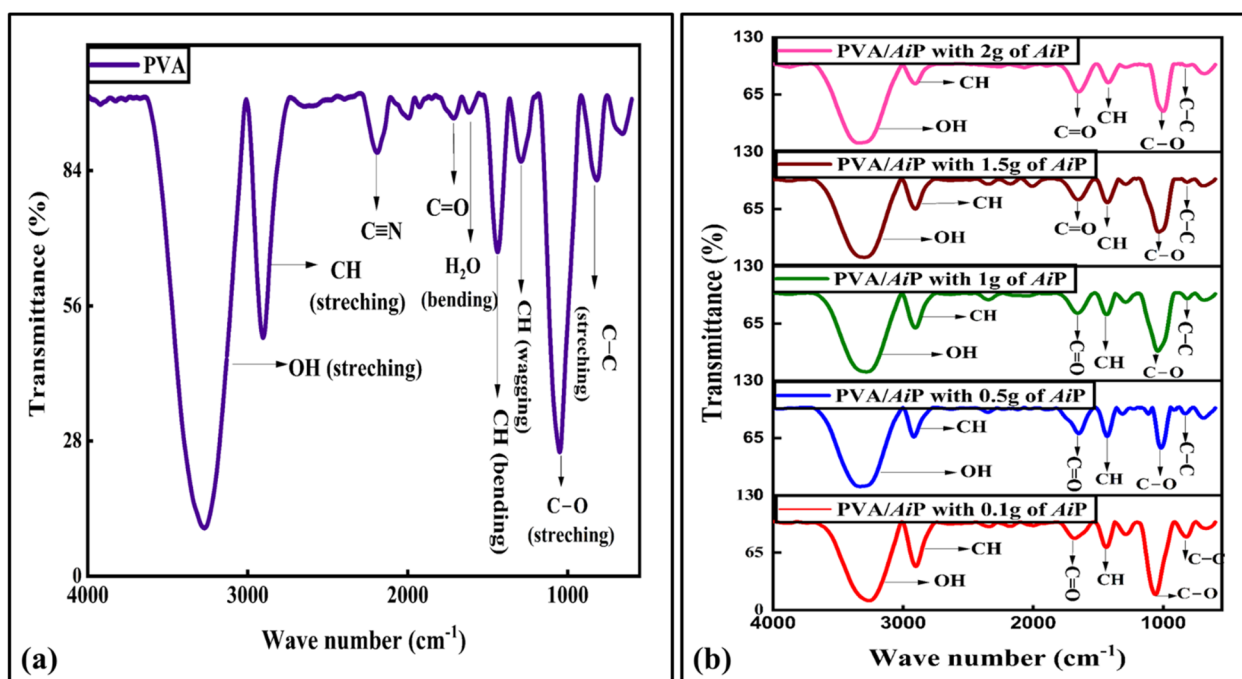


Fig. 2 FTIR spectra of matrix PVA (a) and PVA/AiP hybrid films (b).



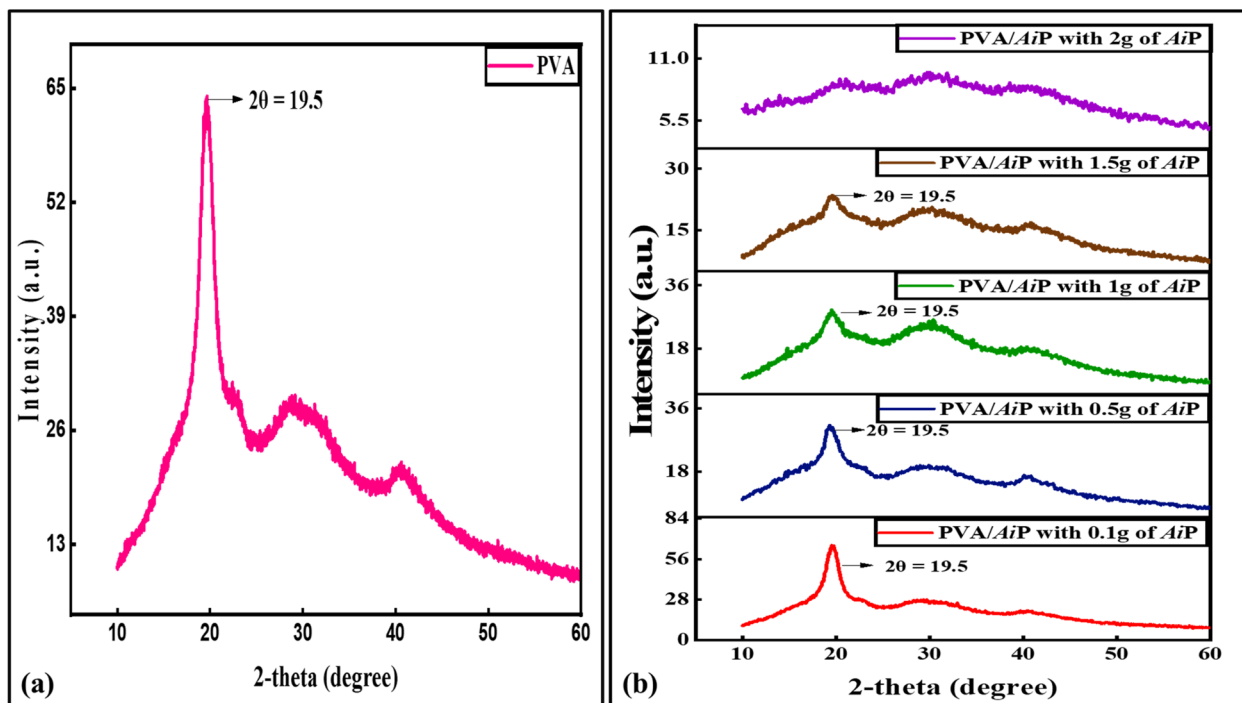


Fig. 3 X-ray diffractogram of matrix PVA (a) and PVA/AiP hybrid films (b).

Table 2 Calculated values of crystallinity index for matrix PVA film and PVA/AiP hybrid films

Sample	Crystallinity index
Matrix PVA	22.13%
0.1 AiP	19.19%
0.5 AiP	14.89%
1.0 AiP	11.30%
1.5 AiP	9.46%
2.0 AiP	7.05%

the FTIR spectra of PVA/AiP hybrid films, the increase in the intensity of the peaks in the range of  $1650\text{--}1700\text{ cm}^{-1}$  with the increase in the concentration of the AiP filler is attributed to the existence of additional carbonyl groups from flavonoids and terpenoids present in the AiP filler. Simultaneously, the intensities of the  $1200\text{--}1400\text{ cm}^{-1}$  and  $2900\text{--}3000\text{ cm}^{-1}$  peaks for  $\text{--CH}$  (bending and wagging) and  $\text{--CH}_2$  stretching decreased when the filler was added, inhibiting the vibrational nature. The higher surface area of AiP causes physical shielding and can alter the polymer chain arrangement, thereby reducing the peak intensity.<sup>30,31</sup> This observation confirms that interactions with AiP can lead to a specific arrangement in PVA/AiP films. Every spectrum of the PVA/AiP hybrid film samples with varying concentrations exhibited remarkably similar peak patterns, with no noticeable differences compared to the pure PVA film, suggesting no chemical interaction between the PVA matrix and filler AiP in the hybrid films. The type of interaction is physical, such as van der Waals, hydrogen bonding, and mechanical interlocking, which results in the enhancement of the thermal and mechanical properties of the PVA/AiP hybrid films.

### 3.2 XRD analysis

X-ray diffractograms of the PVA matrix and hybrid films with varying concentrations of AiP are shown in (Fig. 3). The X-ray diffractogram of the PVA matrix shows a sharp peak at  $2\theta = 19.6^\circ$  (101),<sup>32,33</sup> indicating the crystalline nature and existence of hydrogen bonding (physical interaction) between the PVA chains and hydroxyl groups of the filler AiP. The wider peak at  $2\theta = 29^\circ$  indicates the existence of an amorphous portion in the PVA matrix, confirming its semicrystalline nature. The increase in the loading of AiP filler to the PVA matrix, resulted in the agglomeration of the filler (same was observed in SEM images) resulting in the decrease in the intensity of the crystalline peak of the PVA matrix  $2\theta = 19.6^\circ$ .

The agglomeration of the AiP filler at higher concentrations led to poor orientation and shadowing of the peaks of the PVA matrix. The solution-casting method of fabrication of the PVA/AiP hybrid films suppressed the crystallinity due to the intercalation effect. The crystallinity of the PVA matrix and PVA/AiP hybrid films was calculated using eqn (4) and is presented in Table 2.

$$\text{Crystallinity index} = \frac{\text{area of the crystalline peak}}{\text{area of all the peaks}} \times 100 \quad (4)$$

The crystallinity index of the matrix PVA film, which was semi-crystalline in nature, was 22.13%, and the loading of the AiP filler decreased the crystallinity of the PVA/AiP hybrid films.

### 3.3 Morphological analysis

Optical microscopy and scanning electron microscopy (SEM) were used to investigate the surface morphology and dispersion



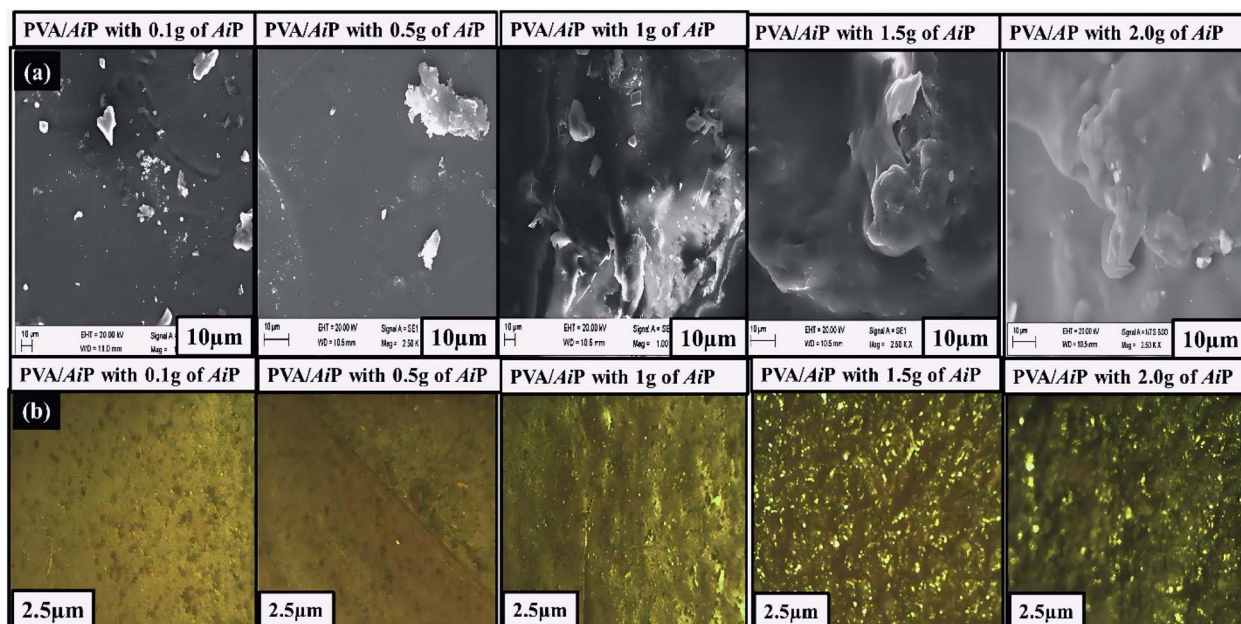


Fig. 4 SEM images (a) and optical microscopy images (b) of PVA/AiP hybrid films.

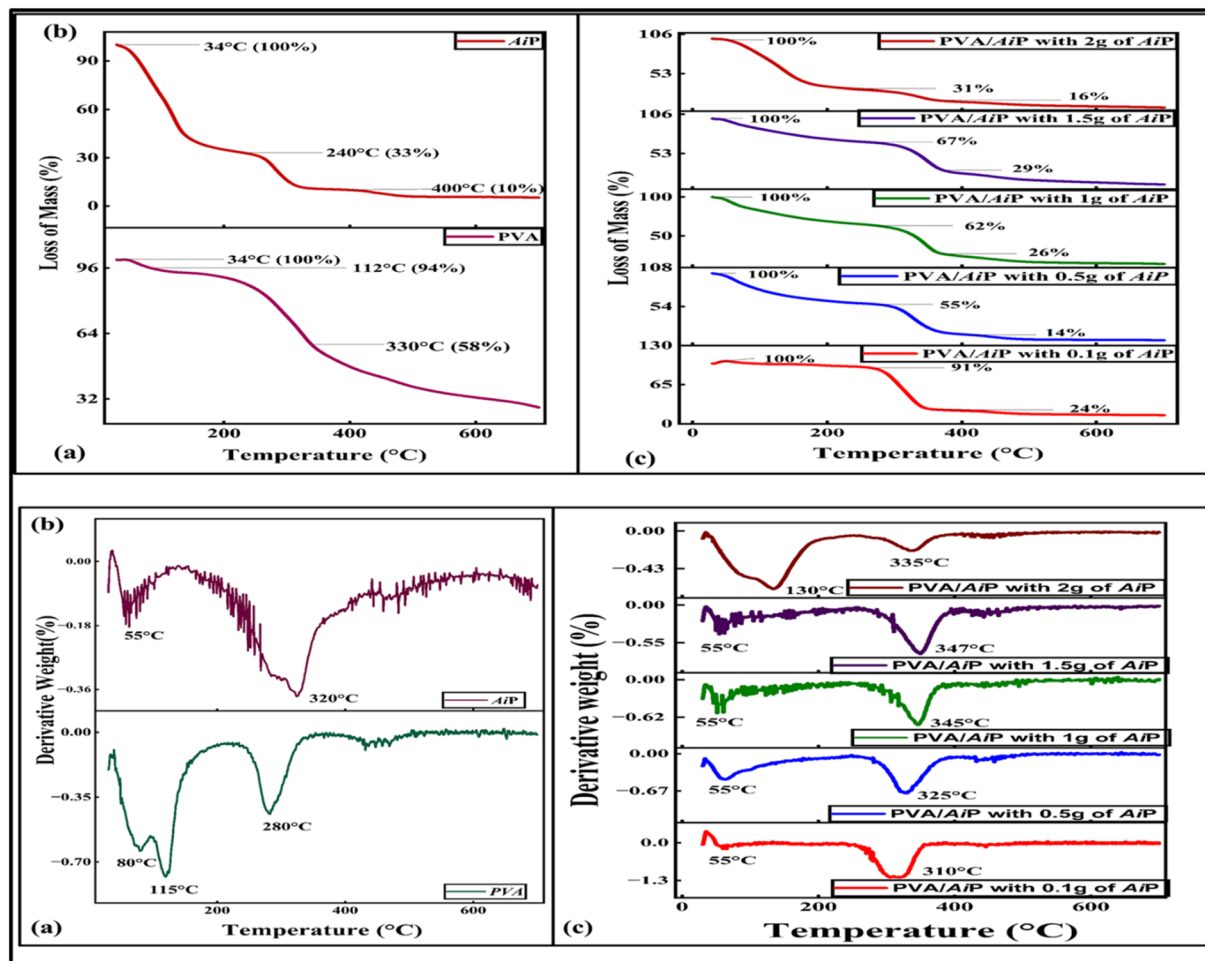


Fig. 5 Primary and derivative thermogram of matrix PVA (a) AiP filler (b) and PVA/AiP hybrid films (c).



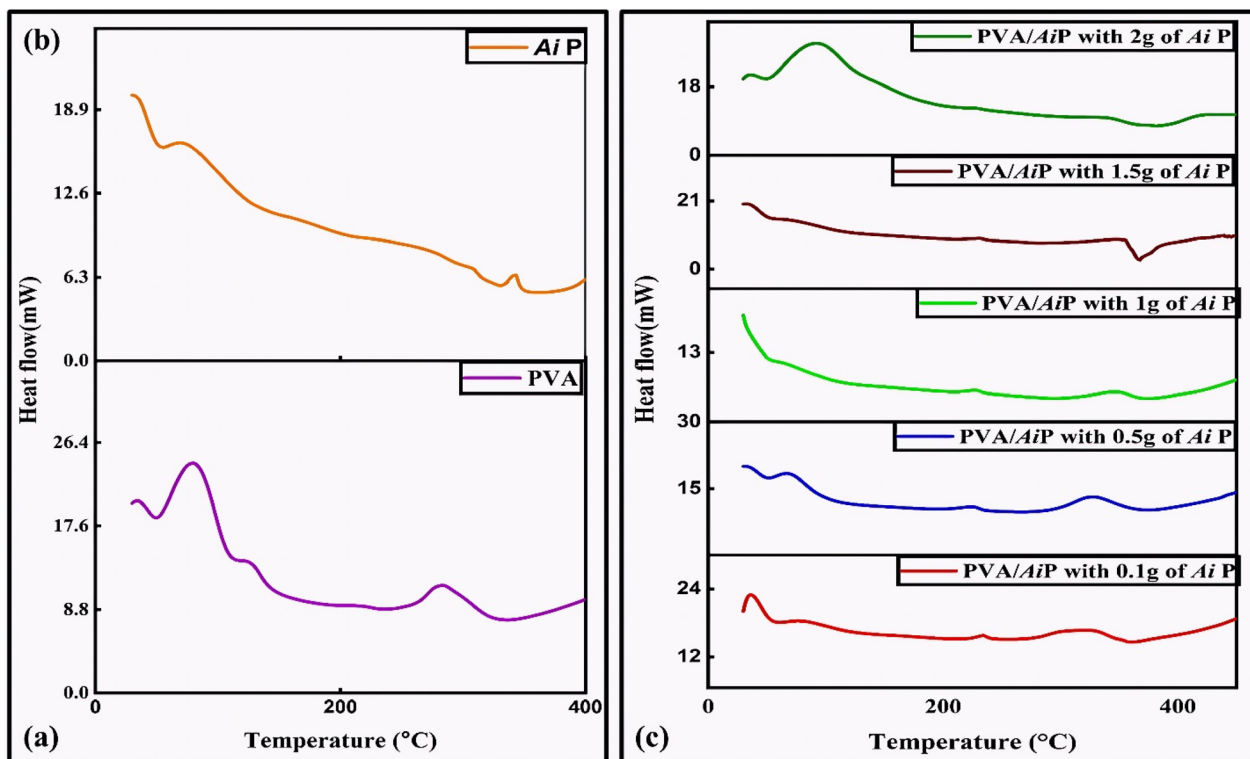


Fig. 6 DSC thermogram of matrix PVA (a) AiP filler (b) and PVA/AiP hybrid films (c).

of the AiP filler in the PVA matrix at various filler concentrations.<sup>1</sup> Both the optical and SEM images indicated a comparatively smooth and uniform surface at low concentrations, with good dispersion and little agglomeration at higher concentrations (Fig. 4). The AiP filler particles became more noticeable at 1.0 g, although the dispersion remained uniform. Particularly in SEM images, noticeable clusters and particle agglomerates were seen when the filler concentration raised to 1.0 g and 1.5 g, suggesting a partial loss of homogeneity. The SEM images showed massive, irregular aggregates and voids at the filler-matrix interface, indicating that the filler was substantially concentrated (2.0 g) and that the surface roughness increased drastically. Overall, the investigation showed that high filler concentrations caused agglomeration and decreased the opacity and transparency, which also affected the mechanical and barrier properties of the film.

### 3.4 Thermogravimetric and differential scanning calorimetry (TGA/DSC) analysis

TGA and DSC were used to analyze the thermal stability of PVA, AiP powder, and PVA/AiP hybrid films, as shown in Fig. 5 and 6. Several phases are involved in the breakdown of the matrix PVA film, as it is hydrophilic in nature. The surface moisture evaporates at 80 °C ( $\approx$ 4% loss), and the bonded water molecules degrade when they come into contact with a hydroxyl group at 115 °C ( $\approx$ 6% loss). Degradation of the polymer chain backbone at 280 °C ( $\approx$ 42% loss) resulted in enormous weight loss. The last loss of char residue occurred at 600 °C ( $\approx$ 95% loss). Moisture is

lost during the thermal degradation of AiP at 55 °C ( $\sim$ 10% loss), and organic contents (cellulose, terpenoids, flavonoids, *etc.*) are lost throughout the majority of the deterioration at 320 °C ( $\sim$ 37% loss). Char residue is lost at 450 °C ( $\approx$ 91% loss), whereas the remaining residue is converted to ash at 600 °C ( $\approx$ 95% loss).<sup>34</sup>

In the case of PVA/AiP hybrid films, the mass loss for moisture occurs at 55 °C for all concentrations, indicating the presence of filler on the PVA/AiP hybrid films. The loading of filler AiP increased the thermal stability of the film. Notably the PVA/AiP hybrid film (with 1 g of PVA and 2.0 g of AiP) undergoes first mass loss at 130 °C, owing to decomposition of its organic contents leaving behind a substantial residue. Additionally, the PVA backbone broke at 335 °C with minimal mass loss, as the quantity of the filler AiP was greater than that of the matrix PVA. The mass of the residue increases as the mass of the filler increases. No additional mass loss region was observed, other

Table 3 Glass transition temperature ( $T_g$ ) and melting temperature ( $T_m$ ), of matrix PVA, filler AiP and PVA/AiP hybrid films

S. no.	Sample	$T_g$ (°C)	$T_m$ (°C)
1	PVA	90	124
2	AiP	310	335
3	PVA/AiP with 0.1 g of AiP	200	235
4	PVA/AiP with 0.5 g of AiP	210	238
5	PVA/AiP with 1 g of AiP	212	240
6	PVA/AiP with 1.5 g of AiP	220	243
7	PVA/AiP with 2 g of AiP	231	332



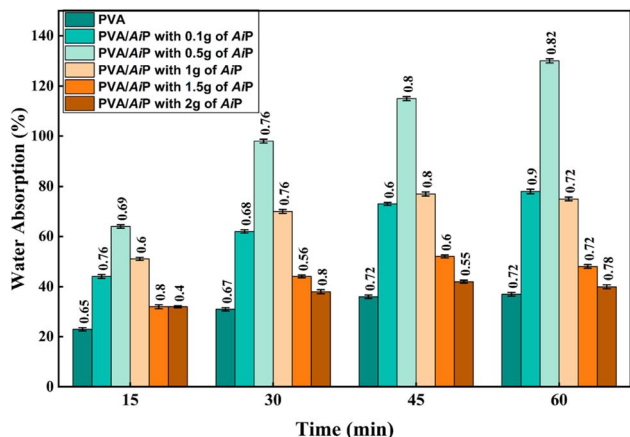


Fig. 7 Results of water absorption of matrix PVA film and PVA/AiP hybrid films.

than the matrix and filler, in the hybrid PVA/AiP films, confirming the existence of only physical interaction between the matrix and the filler AiP, which is in line with the FTIR and XRD analyses.<sup>35</sup>

The thermal behavior of the matrix PVA, filler AiP, and PVA/AiP hybrid films was evaluated using Differential Scanning Calorimetry (DSC), as shown in Fig. 6. The corresponding glass transition temperature ( $T_g$ ) and melting temperature ( $T_m$ ) are listed in Table 3. The DSC thermogram of the PVA matrix exhibited a clear glass transition at approximately 90 °C and a melting temperature of approximately 124 °C, which are typical for semi-crystalline PVA. In contrast, the filler AiP showed significantly higher  $T_g$  and  $T_m$  at 310 °C and 335 °C, respectively, indicating its high thermal stability and rigid molecular structure. Upon the incorporation of the filler AiP into the PVA matrix, a marked enhancement in the thermal transitions was observed. The  $T_g$  of the hybrid films increased progressively from 200 °C (for 0.1 g AiP) to 231 °C (for 2 g AiP), while the  $T_m$  increased from 235 °C to 332 °C over the same range. This upward shift in both  $T_g$  and  $T_m$  can be attributed to strong intermolecular interactions and the effective interfacial compatibility between the PVA matrix and the filler AiP. The restricted mobility of the PVA chains owing to the presence of AiP particles likely contributed to the observed increase in the glass transition temperature. Furthermore, the increase in  $T_m$  suggests that AiP may act as a nucleating agent, enhancing thermal ordering within the PVA matrix. At higher AiP loadings, the thermal profile of the hybrid films began to resemble that of the filler AiP, suggesting a dominant influence of the filler phase. These results demonstrate that the addition of AiP significantly improved the thermal stability of PVA, making the hybrid films more suitable for applications involving elevated temperatures.

### 3.5 Results of water absorption of matrix PVA film and PVA/AiP hybrid films

The water absorption performance of the matrix PVA film and PVA/AiP hybrid films was investigated over a duration of 15–

60 min, and the results are illustrated in Fig. 7. The pure PVA film exhibited the lowest water absorption values across all the time intervals, with a gradual increase from approximately 25% at 15 min to approximately 38% at 60 min. This behaviour is characteristic of the semi-crystalline nature of PVA, which limits water uptake owing to its dense polymeric structure. The incorporation of the filler AiP into the PVA matrix significantly enhanced the water absorption capacity of the resulting hybrid films.<sup>36</sup>

Notably, the film containing 0.5 g of AiP demonstrated the highest water absorption at all time points, reaching a peak of around 130% after 60 minutes. This marked increase can be attributed to the hydrophilic nature of the AiP filler, which promotes water penetration and retention within the polymer network. Films with other AiP loadings (0.1, 1.0, 1.5, and 2.0 g) exhibited intermediate absorption behaviour. The film with 1.0 g of AiP achieved around 80% absorption at 60 minutes, while higher loadings (1.5 g AiP) showed a slight reduction in absorption efficiency compared to the 0.5 g and 1.0 g formulations. At an AiP loading of 2.0 g, the film exhibited very low absorption, which can be attributed to its pronounced brittleness, as discussed in Section 3.7. This behaviour is not typical of films with lower AiP concentrations and highlights that excessive AiP content compromises the structural integrity of the film, thereby affecting its barrier performance. This decline may be attributed to filler agglomeration at higher concentrations, which can reduce the effective surface area for water interactions and potentially hinder the diffusion of water molecules through the film matrix. Overall, the results indicate that the addition of neem leaf powder enhances the hydrophilicity in low concentration and hydrophobicity in higher concentration of the PVA films, with AiP (0.5 g) being the optimal concentration for maximum water absorption. Beyond this concentration, the saturation effect and possible phase separation or filler clustering may reduce the water uptake. For food packaging applications low absorption is more suitable, so 1.5 g has optimal concentration for carried the application process.

### 3.6 Results of oxygen permeability of matrix PVA film and PVA/AiP hybrid films

The oxygen permeabilities of the PVA and PVA/AiP hybrid films were evaluated by measuring the dissolved oxygen (DO) concentration in  $\text{mg L}^{-1}$  over a period of 72 h, as shown in Fig. 8. In general, an increase in the DO concentration over time indicates higher oxygen permeability through the film matrix. The pure PVA film exhibited moderate DO levels, starting at  $\sim 5.5 \text{ mg L}^{-1}$  after 24 h and gradually increasing to  $\sim 7.0 \text{ mg L}^{-1}$  after 72 h. This is consistent with the semi-permeable nature of PVA, which allows the limited diffusion of oxygen owing to its compact polymeric structure.<sup>2</sup>

The incorporation of the filler AiP into the PVA matrix significantly influenced oxygen permeability. The hybrid films containing 0.5 g of AiP showed the highest DO values among the PVA/AiP loaded hybrid films, reaching  $\sim 8.0 \text{ mg L}^{-1}$  at 72 h. This suggests an increase in film porosity and permeability due to the dispersion of the filler AiP, which may disrupt the polymer



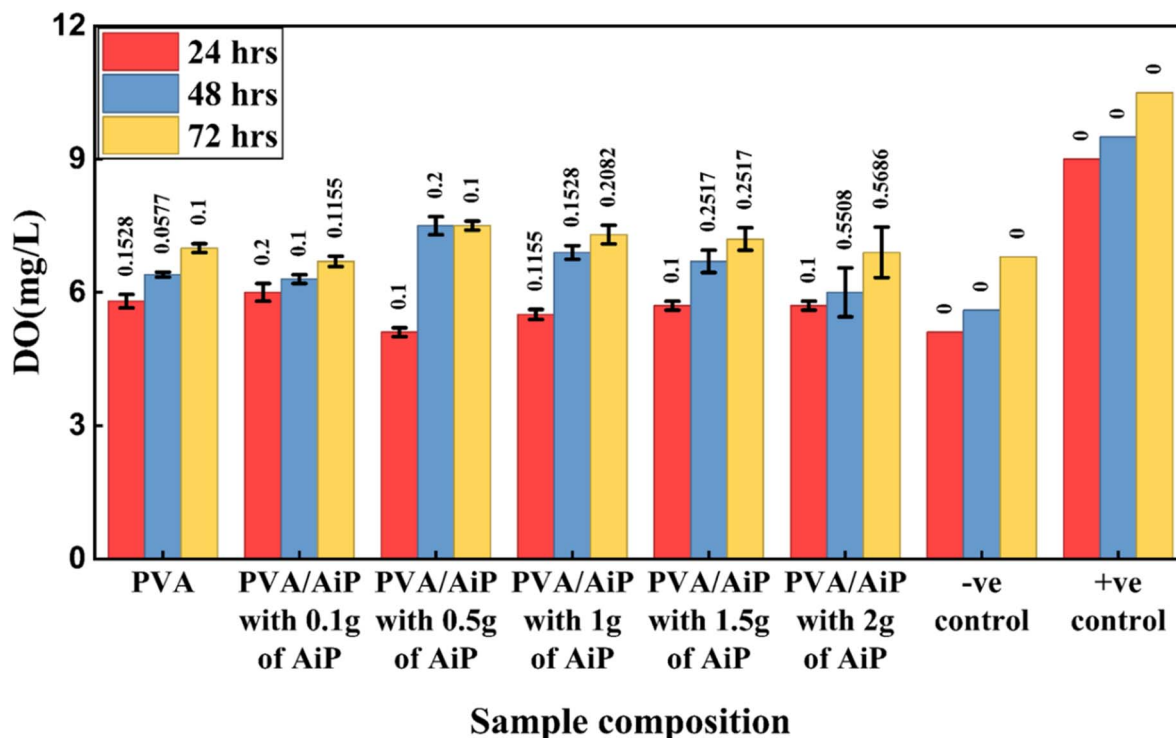


Fig. 8 Results of oxygen permeability test for matrix PVA film and PVA/AiP hybrid films.

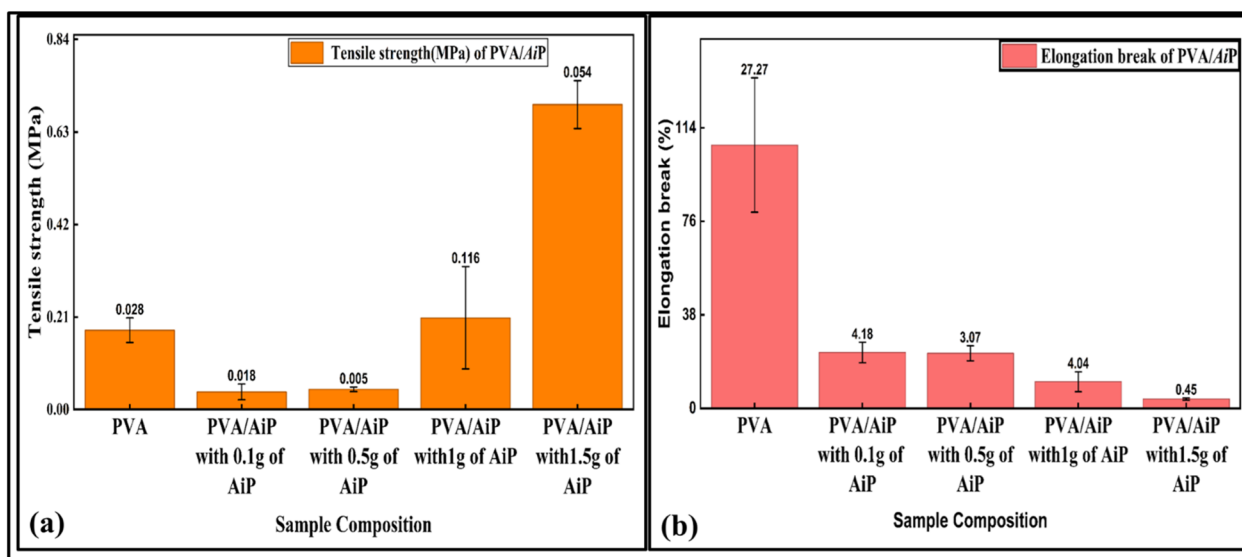


Fig. 9 Tensile strength (a) and elongation at break (b) for matrix PVA film and PVA/AiP hybrid films.

matrix and create microchannels for oxygen diffusion. A similar trend was observed for (1.0 g) and AiP films (1.5 g), although the increase in DO was slightly less pronounced compared to the 0.5 g formulation, which may be due to the agglomeration of the filler at higher concentrations. The film with the highest AiP concentration (2.0 g) showed a slight decline in DO levels, likely due to its pronounced brittleness (Sections 3.5 and 3.7), which reduced oxygen permeability. This behavior is atypical and not directly comparable with films of lower AiP concentrations,

highlighting the adverse impact of excessive loading on barrier and mechanical properties. The positive control (presumably a highly permeable standard) showed the highest DO levels, exceeding  $10 \text{ mg L}^{-1}$  at 72 h, whereas the negative control (likely a highly impermeable material) maintained lower DO levels throughout the testing period. These controls validated the sensitivity of the test method and confirmed the moderate-to-high permeability characteristics of the hybrid films relative to the standard references. Overall, the data indicate that the

**Table 4** Tensile strength and elongation at break of matrix PVA, filler AiP and PVA/AiP hybrid films

S. no.	Sample	Tensile strength (MPa)	Elongation break (%)
1	PVA	0.18	106.96
2	PVA/AiP with 0.1 g of AiP	0.040	22.66
3	PVA/AiP with 0.5 g of AiP	0.046	22.40
4	PVA/AiP with 1 g of AiP	0.208	10.84
5	PVA/AiP with 1.5 g of AiP	0.692	3.78
6	PVA/AiP with 2 g of AiP	18.82	20.54

incorporation of neem leaf powder enhances the oxygen permeability of the PVA films, with an optimal effect observed at 0.5 g Ai loading. In 1.5 g and 2 g AiP content shows less oxygen permeability, this could be advantageous for specific applications such as dry food packaging, where controlled oxygen transfer is desirable.

Overall, the data indicate that the incorporation of neem leaf powder enhances the oxygen permeability of the PVA films, with an optimal effect observed at 0.5 g AiP loading. While increased oxygen permeability may be undesirable in conventional barrier packaging, it can be advantageous in specific active packaging applications. For instance, respiring fresh produce such as fruits and vegetables require controlled oxygen transfer to maintain aerobic respiration and prevent anaerobic spoilage.<sup>37</sup> Additionally, oxygen-permeable films can enhance the performance of embedded oxygen scavengers or antimicrobial agents—such as those derived from neem—by facilitating interaction with ambient oxygen.<sup>38</sup> In certain systems, moderate

oxygen ingress can also help modulate microbial activity and enzymatic processes, contributing to shelf-life extension and product stability.<sup>39</sup> These findings suggest that the 0.5 g AiP formulation may be particularly suitable for active packaging designs that benefit from controlled oxygen exchange.

### 3.7 Mechanical strength

The mechanical strengths of the matrix PVA film and PVA/AiP hybrid films were analyzed and are presented in Fig. 9 and Table 3. The PVA matrix exhibited a modest tensile strength approximately 0.23 MPa, which was typical of its soft and flexible polymeric structure. There was a progressive increase in the tensile strength with the gradual addition of AiP (from 0.1 to 1.5 g), with a significant increase observed at higher loadings.<sup>40</sup> The most notable enhancement occurred at 2 g of AiP, where the tensile strength reached 18.82 MPa representing an approximately 82-fold improvement compared to pure PVA (Table 4). This significant reinforcement effect was attributed to the dominance of the rigid filler phase in the hybrid structure. At this high loading (PVA : AiP = 1 : 2), the AiP particles were well-dispersed and tightly packed within the polymer matrix, forming a stiff network that efficiently transferred the applied stress. Moreover, strong filler–matrix interactions likely contributed to the improved mechanical integrity, converting it from a flexible film into a structurally rigid material.

In contrast, the elongation at break sharply decreased with increasing AiP content. While the PVA matrix PVA showed excellent ductility, with elongation exceeding 120%, all PVA/AiP hybrid films exhibited significantly reduced stretchability. At 2 g of AiP, the elongation decreased to near-zero, indicating

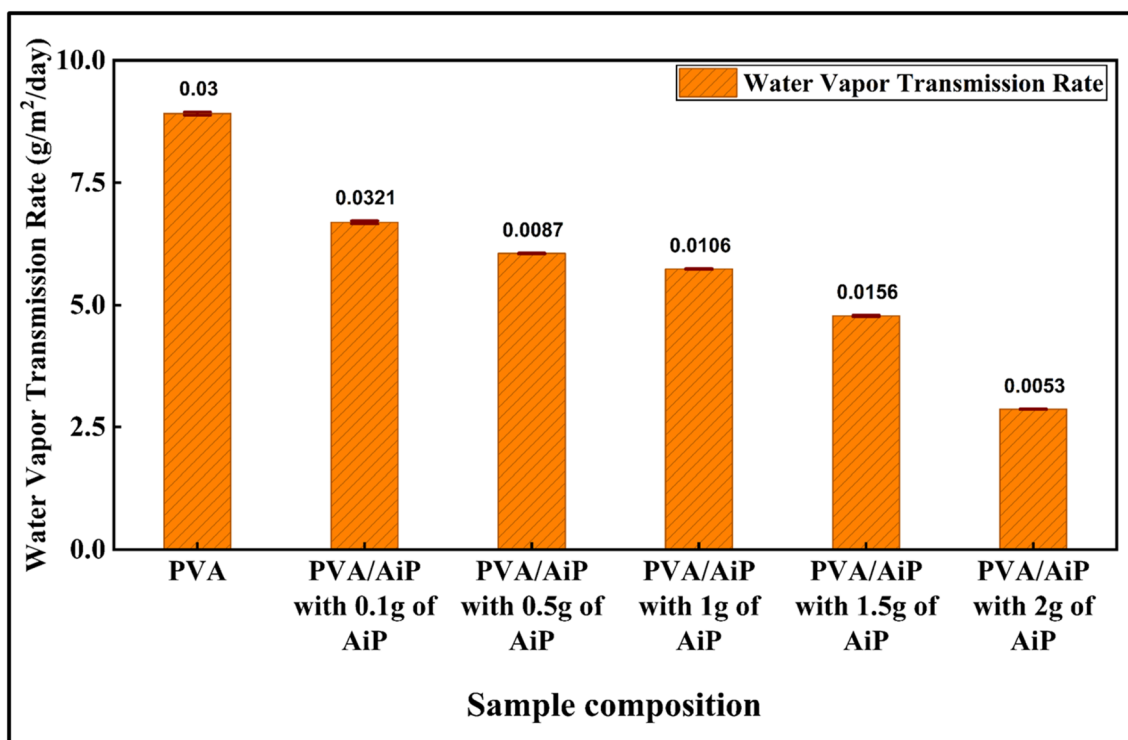


**Fig. 10** Water vapour transmission rate for matrix PVA film and PVA/AiP hybrid films.



extreme brittleness.<sup>24</sup> This reduction results from the restriction of the polymer chain mobility due to the high volume fraction of the rigid filler. At such a high filler content, the polymer matrix is constrained and can no longer accommodate deformation under stress, leading to brittle fracture.

### 3.8 Results of water vapour transmission rate (WVTR)

The water vapour transmission rate (WVTR) of matrix PVA and PVA/AiP hybrid films with increasing filler content (0.1 g to 2.0 g of AiP for 1 g of PVA) is illustrated in Fig. 10. The PVA matrix exhibited a high WVTR ( $\sim 8.8 \text{ g m}^{-2} \text{ day}^{-1}$ ), indicative of its hydrophilic nature and relatively open polymeric structure, which facilitated the diffusion of water molecules through the film matrix. Upon incorporation of AiP, a consistent and progressive reduction in the WVTR was observed with increasing filler loading. At 0.1 g and 0.5 g of AiP, the WVTR values dropped moderately, reflecting the partial obstruction of water molecule pathways by the dispersed filler particles. As the filler content increased further to 1.0 g and 1.5 g, a more pronounced decline in WVTR was noted, suggesting improved barrier properties due to enhanced tortuosity and reduced free volume within the polymer matrix.

The most significant reduction occurred with 2.0 g of AiP, where the WVTR reached a minimum value of approximately  $2.8 \text{ g m}^{-2} \text{ day}^{-1}$ . This dramatic drop ( $\sim 68\%$  reduction compared to pure PVA) can be attributed to the dense filler network and strong matrix-filler interactions, which hindered the diffusion of water vapor through the film. The presence of high amounts of inorganic AiP likely contributed to a more compact microstructure, thereby effectively acting as a moisture barrier. The decreasing trend in WVTR with increasing AiP content confirms that filler incorporation significantly enhances the water vapor barrier performance of the PVA films. The 2.0 g AiP film exhibited a lower WVTR value, which can be attributed to its increased and non-uniform thickness compared to the lower concentration films (Table 1). This variation in thickness, combined with the film's brittleness, influenced its moisture barrier performance, highlighting the importance of controlling both film uniformity and composition for optimal WVTR behavior. These results suggest that PVA/AiP composites, particularly at higher filler loadings (e.g., 1.5 g of AiP), are well-suited for applications in moisture-sensitive packaging and environmentally responsive coatings, where reduced water permeability is critical.

### 3.9 Soil degradability

The soil degradation behavior of the PVA/AiP hybrid films demonstrated a non-linear pattern in correlation with the concentration of the AiP filler (Fig. 11). In comparison to the PVA films, the film containing (0.1 g) showed a faster rate of degradation. This suggests that a small amount of AiP can improve biodegradability by improving the film porosity and decreasing crystallinity, which facilitates simpler microbial penetration. At increasing neem concentrations (0.5 g, 1 g, 1.5, and 2 g of AiP), the rate of breakdown dramatically decreased. The hydrophobic properties of neem and antibacterial

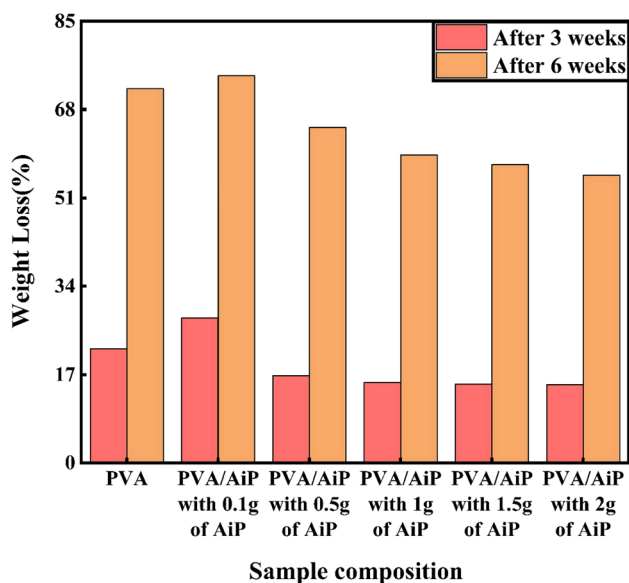


Fig. 11 Soil biodegradability data for matrix PVA film and PVA/AiP hybrid films.

chemicals are thought to be responsible for this decrease, as they probably prevent microbial activity and lower water absorption. Additionally, too much neem may make the film denser and stiffer, preventing microbiological decomposition. As a result, whereas greater loadings restrict biodegradability, low concentrations of AiP (0.1 g of AiP) encourage decomposition, making filler content optimization essential for environmentally friendly packaging applications.

The weight loss (%) of matrix PVA and PVA/AiP hybrid films after 3 and 6 weeks of soil degradation is given in Table 4. After six weeks of soil degradation, the highest weight loss was measured for the specimens PVA/AiP with 0.1 g of AiP while the lowest weight loss was found in the specimens PVA/AiP with 2 g of AiP. The soil degradation of the specimens decreased with the increase of the AiP (Table 5).

### 3.10 Results of antimicrobial analysis

The matrix PVA film shows no inherent antibacterial activity, but adding AiP enhances their efficacy in a concentration-dependent manner (Fig. 12). Low concentrations (0.1 g AiP) have minimal effect, while higher concentrations (1.5 g AiP) show stronger inhibition against *E. coli*. The study emphasizes

Table 5 Weight loss (%) of matrix PVA and PVA/AiP hybrid films after 3 and 6 weeks of soil degradation

S. no.	Sample	After three weeks weight loss (%)	After six weeks weight loss (%)
1	PVA	22.2%	72%
2	PVA/AiP with 0.1 g of AiP	27.9%	74.5%
3	PVA/AiP with 0.5 g of AiP	16.8%	64.6%
4	PVA/AiP with 1 g of AiP	15.5%	59.3%
5	PVA/AiP with 1.5 g of AiP	15.2%	57.4%
6	PVA/AiP with 2 g of AiP	15.1%	55.4%



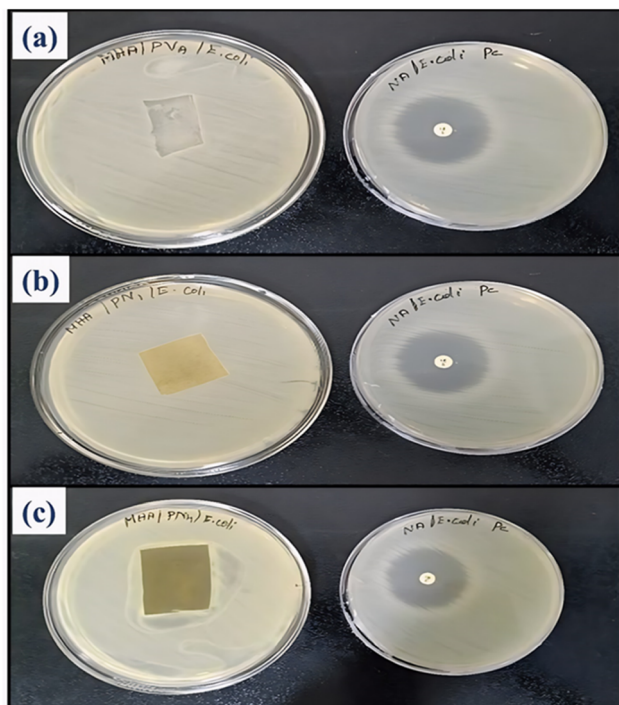


Fig. 12 Antimicrobial activity of PVA film (a), PVA/AiP with 0.1 g of AiP (b), PVA/AiP with 1.5 g of AiP (c) against *E. coli*.

the importance of balancing antimicrobial effectiveness with film structure and permeability. The disk diffusion method used provides reliable results, demonstrating the enhanced

Table 6 Area of inhibition zone for PVA and PVA/AiP film for *E. coli*

S. no.	Samples	Area of inhibition for <i>E. coli</i> (cm <sup>2</sup> )
1	PVA	—
2	PVA/AiP with 0.1 g of AiP	0.03
3	PVA/AiP with 1.5 g of AiP	7.06

antibacterial performance of PVA/AiP hybrid films. These findings have implications for developing antimicrobial packaging materials, with potential applications in food packaging and medical supplies. The research suggests future directions, including optimizing AiP concentration, investigating long-term stability, and evaluating effectiveness against various microorganisms (Fig. 13).

The area of inhibition zone for PVA and PVA/AiP film for *E. coli* is given in Table 6. The area of the inhibition zone sharply increased from 0.03 to 7.06 cm<sup>2</sup> when the amount of the AiP increased from 0.1 to 1.5 g of AiP.

#### 4 PVA/AiP hybrid films as an active packaging material for cowpeas

This study demonstrates the potential of PVA/AiP hybrid films for dry food packaging applications, particularly in extending the shelf life of cowpeas under ambient conditions. Approximately 5 g of dry cowpeas were wrapped using matrix PVA film and PVA/AiP hybrid film, each measuring 8 × 8 cm. An equal quantity of cowpeas was left exposed to open air as a negative

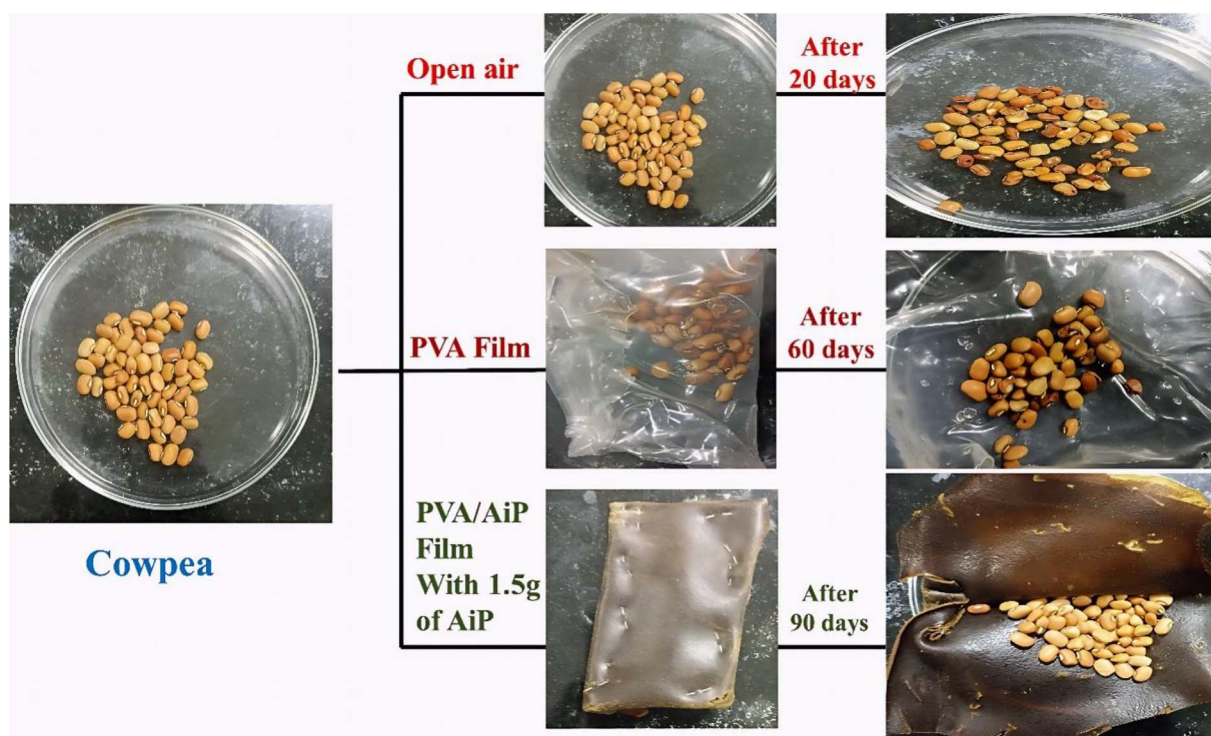


Fig. 13 Packaging application of PVA and PVA/AiP hybrid films to cowpeas.



Table 7 Summary of optimal AiP loadings for key functional properties

Property	Optimal AiP loading	Observed effect
Water absorption	0.5 g	Highest uptake (~130% at 60 min); enhanced hydrophilicity due to filler dispersion
Oxygen permeability	0.5 g	Increased permeability; filler promotes porosity and water interaction
Tensile strength	2.0 g	Maximum mechanical strength; dense filler phase reinforces matrix
Water vapor transmission rate (WVTR)	2.0 g	Lowest WVTR; reduced moisture permeability due to compact structure
Soil degradability	0.1 g	Fastest degradation; minimal filler allows rapid breakdown
Antimicrobial activity	1.5 g	Strongest inhibition zone; sufficient bioactive content with good dispersion

Table 8 Comparison of PVA/AiP films with bio-based and commercial packaging materials

Film type/material	Tensile strength (MPa)	Elongation at break (%)	WVTR (g mm m <sup>-2</sup> day <sup>-1</sup> kPa <sup>-1</sup> )	Additional features
Starch/PVA blend	14.5 ± 0.6	22.0 ± 1.5	5.8	Biodegradable, moderate barrier
Active PLA-based films (chitosan/essential oils)	20–25	10–15	2.5–3.0	Antimicrobial, biodegradable
<b>Turmeric extract in PVA</b>	15.2 ± 0.8	18.5 ± 1.2	4.5–5.0	Moderate antimicrobial vs. <i>E. coli</i>
<b>Neem extract in PVA</b>	17.0 ± 0.9	19.2 ± 1.0	3.8–4.2	Strong antimicrobial vs. Gram-positive & Gram-negative
Commercial LDPE (food packaging)	8–12	100–500	12–20	Excellent flexibility, poor moisture barrier
Commercial PET (food packaging)	55–75	80–120	2.0–3.0	Strong, durable, widely used, non biodegradable
<b>Present work PVA/AiP</b>	<b>18.82 ± 0.9</b>	<b>20.54 ± 1.1</b>	<b>2.8</b>	Balanced mechanical, WV barrier & antimicrobial, biodegradable

control. Over a 90 days observation period, the cowpeas stored in open air showed fungal growth, discoloration, and physical deterioration within 20 days. Those wrapped in matrix PVA film exhibited moderate protection, extending shelf life to around 60 days. In contrast, cowpeas packaged in the PVA/AiP hybrid film remained fresh, free from discoloration, unpleasant odors, and fungal spots for up to 90 days. This preservation is attributed to the antimicrobial and antifungal properties of *Azadirachta indica* powder (AiP), which inhibited microbial growth.<sup>35</sup> A summary of optimal AiP loadings for each evaluated property is presented in Table 7, to highlight the trade-offs and guide formulation decisions.

The 1.5 g AiP formulation was selected for packaging trials based on its balanced performance across key functional parameters. While other concentrations may have excelled in isolated properties such as water absorption or oxygen permeability, the 1.5 g loading provided optimal barrier integrity, thermal stability, mechanical strength, and antimicrobial efficacy—making it the most suitable candidate for real-world application.

Furthermore, neem leaf powder is an agro-waste material that is abundant, renewable, and low-cost. Its incorporation partially replaces synthetic polymer content, which may contribute to reduced material costs and improved sustainability. A comparison of developed PVA/AiP hybrid films with other commercially available polymers were presented in Table 8. In summary, PVA/AiP hybrid films offer a promising

multifunctional platform for active food packaging, combining structural integrity with microbial resistance.

## 5 Conclusions

The PVA/AiP hybrid films were successfully fabricated through a solution-casting method, incorporating different amounts of AiP as a bio-filler. Extensive analysis was conducted using a range of analytical techniques. The findings indicated a physical interaction between PVA and AiP, with effective filler dispersion at lower concentrations and clumping at higher levels. As the AiP content increased, the hybrid films demonstrated enhanced thermal stability, water absorption, oxygen permeability, tensile strength, and antimicrobial properties. However, the films' elongation at break decreased, and soil degradability improved only at low AiP concentrations. The PVA/AiP hybrid films were effective at extending the shelf life of dry cowpeas by approximately 90 days when used as active packaging. The results highlight the potential of PVA/AiP hybrid films as sustainable, efficient, active food packaging materials that align with SDG 12 by promoting responsible consumption and production. The fabricated PVA/AiP hybrid films are biodegradable and cost-effective to produce.

## Ethics approval

No human and/or animal studies were used in this article, and all authors are fully aware that nothing in this article violates ethics.



## Author contributions

TamilAnand Solaikannan and Sivaranjana Paramasivan designed the experiments, performed data acquisition, and contributed to data analysis and interpretation. TamilAnand Solaikannan drafted the initial manuscript and prepared the figures. Rajini Nagarajan and Nadir Ayrlmis critically revised the manuscript for intellectual content, enhancing technical accuracy and structural coherence. All authors reviewed and endorsed the submitted manuscript.

## Conflicts of interest

The authors declare no conflicts of interest.

## Data availability

Data will be made available on request.

Supplementary information is available. See DOI: <https://doi.org/10.1039/d5ra05486a>.

## Acknowledgements

This research received no specific grant from any funding agency in the public, commercial, or not-for-profit sectors.

## References

- 1 H. Abrial, A. Atmajaya, M. Mahardika, F. Hafizulhaq, Kadriadi, D. Handayani, S. M. Sapuan and R. A. Ilyas, Effect of ultrasonication duration of polyvinyl alcohol (PVA) gel on characterizations of PVA film, *J. Mater. Res. Technol.*, 2020, **9**, 2477–2486, DOI: [10.1016/j.jmrt.2019.12.078](https://doi.org/10.1016/j.jmrt.2019.12.078).
- 2 L. Zhang, J. Cai, K. O. Reddy, A. V. Rajulu, J. Duan and B. Ashok, Effects of spent tea leaf powder on the properties and functions of cellulose green composite films, *J. Environ. Chem. Eng.*, 2015, **4**, 440–448, DOI: [10.1016/j.jece.2015.11.029](https://doi.org/10.1016/j.jece.2015.11.029).
- 3 P. Phansamarn, A. Bacchus, F. Hassan Pour, C. Kongvarhodom and P. Fatehi, Cationic lignin incorporated polyvinyl alcohol films for packaging applications, *Ind. Crops Prod.*, 2024, **221**, 119217, DOI: [10.1016/j.indcrop.2024.119217](https://doi.org/10.1016/j.indcrop.2024.119217).
- 4 J. Y. Tan, W. Y. Tey, J. Panpranot, S. Lim and K. M. Lee, Valorization of Oil Palm Empty Fruit Bunch for Cellulose Fibers: A Reinforcement Material in Polyvinyl Alcohol Biocomposites for Its Application as Detergent Capsules, *Sustainability*, 2022, **14**, 11446, DOI: [10.3390/su141811446](https://doi.org/10.3390/su141811446).
- 5 V. A. Pereira, I. N. Q. de Arruda and R. Stefani, Active chitosan/PVA films with anthocyanins from Brassica oleraceae (Red Cabbage) as Time-Temperature Indicators for application in intelligent food packaging, *Food Hydrocolloids*, 2015, **43**, 180–188, DOI: [10.1016/j.foodhyd.2014.05.014](https://doi.org/10.1016/j.foodhyd.2014.05.014).
- 6 R. M. Rowell, A. R. Sanadi, D. F. Caulfield and R. E. Jacobson, Utilization of Natural Fibers in Plastic Composites: Problems and Opportunities, Lignocellulosic-Plastic Composites, *Ind. Eng. Chem. Res.*, 1997, 23–51.
- 7 H. Deng, J. Su, W. Zhang, A. Khan, M. A. Sani, G. Goksen, P. Kashyap, P. Ezati and J. W. Rhim, A review of starch/polyvinyl alcohol (PVA) blend film: A potential replacement for traditional plastic-based food packaging film, *Int. J. Biol. Macromol.*, 2024, **273**, 132926, DOI: [10.1016/J.IJBIOMAC.2024.132926](https://doi.org/10.1016/J.IJBIOMAC.2024.132926).
- 8 M. C. Alvarado, Recent progress in polyvinyl alcohol (PVA)/nanocellulose composite films for packaging applications: A comprehensive review of the impact on physico-mechanical properties, *Food Bioeng.*, 2024, **3**, 189–209, DOI: [10.1002/fbe2.12086](https://doi.org/10.1002/fbe2.12086).
- 9 S. Achutha, S. Kumari Nisha, Sr. Barakala Pushpa and S. Andrews, Antimicrobial polyvinyl alcohol/neem oil flexible film for food packaging applications, *Mater. Today: Proc.*, 2023, DOI: [10.1016/j.matpr.2023.07.061](https://doi.org/10.1016/j.matpr.2023.07.061).
- 10 A. Ali, M. A. Shahid, M. D. Hossain and M. N. Islam, Antibacterial bi-layered polyvinyl alcohol (PVA)-chitosan blend nanofibrous mat loaded with *Azadirachta indica* (neem) extract, *Int. J. Biol. Macromol.*, 2019, **138**, 13–20, DOI: [10.1016/j.ijbiomac.2019.07.015](https://doi.org/10.1016/j.ijbiomac.2019.07.015).
- 11 R. Subapriya and S. Nagini, Medicinal Properties of Neem Leaves : A Review, *Curr. Med. Chem.: Anti-Cancer Agents*, 2005, 149–156.
- 12 G. Srisugamathi, A. Thirumurugan, A. V. Samrot, P. Sengupta, S. Dutta and R. R. Remya, Development of nanocellulose-based composite derived from wood waste of *Azadirachta indica* for food packaging application, *Biomass Convers. Biorefin.*, 2023, 25083–25091, DOI: [10.1007/s13399-023-04733-5](https://doi.org/10.1007/s13399-023-04733-5).
- 13 S. A. Riyajan and J. T. Sakdapipanich, Characterization of biodegradable semi-interpenetrating polymer based on poly(vinyl alcohol) and sodium alginate containing natural neem (*Azadirachta indica*) for controlled release application, *Polym. Int.*, 2010, **59**, 1130–1140, DOI: [10.1002/pi.2839](https://doi.org/10.1002/pi.2839).
- 14 M. T. Hossain and M. A. Shahid, Fabrication of antibacterial bio-composite from polyvinyl alcohol incorporated with *Azadirachta indica*, *SPE Polym.*, 2024, **6**, e10156, DOI: [10.1002/pls2.10156](https://doi.org/10.1002/pls2.10156).
- 15 H. Wen, Y. I. Hsu, T. A. Asoh and H. Uyama, Antioxidant activity and physical properties of pH-sensitive biocomposite using poly(vinyl alcohol) incorporated with green tea extract, *Polym. Degrad. Stab.*, 2020, **178**, 109215, DOI: [10.1016/j.polymdegradstab.2020.109215](https://doi.org/10.1016/j.polymdegradstab.2020.109215).
- 16 S. Singh, K. K. Gaikwad and Y. S. Lee, Antimicrobial and antioxidant properties of polyvinyl alcohol bio composite films containing seaweed extracted cellulose nano-crystal and basil leaves extract, *Int. J. Biol. Macromol.*, 2018, **107**, 1879–1887, DOI: [10.1016/j.ijbiomac.2017.10.057](https://doi.org/10.1016/j.ijbiomac.2017.10.057).
- 17 A. Ali, M. A. Shahid, M. D. Hossain and M. N. Islam, Antibacterial bi-layered polyvinyl alcohol (PVA)-chitosan blend nanofibrous mat loaded with *Azadirachta indica* (neem) extract, *Int. J. Biol. Macromol.*, 2019, **138**, 13–20, DOI: [10.1016/j.ijbiomac.2019.07.015](https://doi.org/10.1016/j.ijbiomac.2019.07.015).



- 18 J. C. Antunes, T. D. Tavares, M. A. Teixeira, M. O. Teixeira, N. C. Homem, M. T. P. Amorim and H. P. Felgueiras, Eugenol-containing essential oils loaded onto chitosan/polyvinyl alcohol blended films and their ability to eradicate staphylococcus aureus or pseudomonas aeruginosa from infected microenvironments, *Pharmaceutics*, 2021, **13**, 195, DOI: [10.3390/pharmaceutics13020195](https://doi.org/10.3390/pharmaceutics13020195).
- 19 Q. Q. Leng, Y. Li, X. L. Pang, B. Q. Wang, Z. X. Wu, Y. Lu, K. Xiong, L. Zhao, P. Zhou and S. Z. Fu, Curcumin nanoparticles incorporated in PVA/collagen composite films promote wound healing, *Drug Delivery*, 2020, **27**, 1676–1685, DOI: [10.1080/10717544.2020.1853280](https://doi.org/10.1080/10717544.2020.1853280).
- 20 L. M. Quintero-Borregales, A. Vergara-Rubio, A. Santos, L. Famá and S. Goyanes, Black Tea Extracts/Polyvinyl Alcohol Active Nanofibers Electrospun Mats with Sustained Release of Polyphenols for Food Packaging Applications, *Polymers*, 2023, **15**(5), 1311, DOI: [10.3390/polym15051311](https://doi.org/10.3390/polym15051311).
- 21 S. Anjimon, R. Sobti, K. A. Jayasheel Kumar, A. Kumar, S. C. Parashar and R. A. Hussien, Revolutionizing Packaging and Consumer Products: Exploring the Potential of Biodegradable Materials, *E3S Web Conf.*, 2024, **472**, 02006, DOI: [10.1051/e3sconf/202447202006](https://doi.org/10.1051/e3sconf/202447202006).
- 22 J. L. Wiles, P. J. Vergano, F. H. Barron, J. M. Bunn and R. F. Testin, Water vapor transmission rates and sorption behavior of chitosan films, *J. Food Sci.*, 2000, **65**, 1175–1179, DOI: [10.1111/j.1365-2621.2000.tb10261.x](https://doi.org/10.1111/j.1365-2621.2000.tb10261.x).
- 23 T. Dong, X. Yun, M. Li, W. Sun, Y. Duan and Y. Jin, Biodegradable high oxygen barrier membrane for chilled meat packaging, *J. Appl. Polym. Sci.*, 2015, **132**, 1–8, DOI: [10.1002/app.41871](https://doi.org/10.1002/app.41871).
- 24 N. Jain, V. K. Singh and S. Chauhan, A review on mechanical and water absorption properties of polyvinyl alcohol based composites/films, *J. Mech. Behav. Mater.*, 2017, **26**, 213–222, DOI: [10.1515/jmbm-2017-0027](https://doi.org/10.1515/jmbm-2017-0027).
- 25 R. Sothornvit and N. Pitak, Oxygen permeability and mechanical properties of banana films, *Food Res. Int.*, 2007, **40**(3), 365–370, DOI: [10.1016/j.foodres.2006.10.010](https://doi.org/10.1016/j.foodres.2006.10.010).
- 26 J. M. Kim, M. H. Lee, J. A. Ko, D. H. Kang, H. Bae and H. J. Park, Influence of Food with High Moisture Content on Oxygen Barrier Property of Polyvinyl Alcohol (PVA)/Vermiculite Nanocomposite Coated Multilayer Packaging Film, *J. Food Sci.*, 2018, **83**, 349–357, DOI: [10.1111/1750-3841.14012](https://doi.org/10.1111/1750-3841.14012).
- 27 N. Abinaya, P. Sivaranjana, N. Rajini and K. Krishnan, Performance analysis of biodegradable composite using polyvinyl alcohol and pomegranate peel powder for sustainable dry packaging applications, *Discover Mater.*, 2024, **4**(1), 63, DOI: [10.1007/s43939-024-00139-w](https://doi.org/10.1007/s43939-024-00139-w).
- 28 R. Hussain, S. A. Batool, A. Aizaz, M. Abbas and M. A. Ur Rehman, Biodegradable Packaging Based on Poly(vinyl Alcohol) and Carboxymethyl Cellulose Films Incorporated with Ascorbic Acid for Food Packaging Applications, *ACS Omega*, 2023, **8**, 42301–42310, DOI: [10.1021/acsomega.3c04397](https://doi.org/10.1021/acsomega.3c04397).
- 29 M. S. Sarwar, M. B. K. Niazi, Z. Jahan, T. Ahmad and A. Hussain, Preparation and characterization of PVA/nanocellulose/Ag nanocomposite films for antimicrobial food packaging, *Carbohydr. Polym.*, 2018, **184**, 453–464, DOI: [10.1016/j.carbpol.2017.12.068](https://doi.org/10.1016/j.carbpol.2017.12.068).
- 30 M. Asad, N. Saba, A. M. Asiri, M. Jawaid, E. Indarti and W. D. Wanrosli, Preparation and characterization of nanocomposite films from oil palm pulp nanocellulose/poly (Vinyl alcohol) by casting method, *Carbohydr. Polym.*, 2018, **191**, 103–111, DOI: [10.1016/j.carbpol.2018.03.015](https://doi.org/10.1016/j.carbpol.2018.03.015).
- 31 G. Açık, M. Kamaci, B. Özata and C. E. Özen Cansoy, Effect of polyvinyl alcohol/chitosan blend ratios on morphological, optical, and thermal properties of electrospun nanofibers, *Turk. J. Chem.*, 2019, **43**, 137–149, DOI: [10.3906/kim-1801-68](https://doi.org/10.3906/kim-1801-68).
- 32 N. M. Deghiedy and S. M. El-Sayed, Evaluation of the structural and optical characters of PVA/PVP blended films, *Opt. Mater.*, 2020, **100**, 109667, DOI: [10.1016/j.optmat.2020.109667](https://doi.org/10.1016/j.optmat.2020.109667).
- 33 H. Abrial, A. Atmajaya, M. Mahardika, F. Hafizulhaq, Kadriadi, D. Handayani, S. M. Sapuan and R. A. Ilyas, Effect of ultrasonication duration of polyvinyl alcohol (PVA) gel on characterizations of PVA film, *J. Mater. Res. Technol.*, 2020, **9**, 2477–2486, DOI: [10.1016/j.jmrt.2019.12.078](https://doi.org/10.1016/j.jmrt.2019.12.078).
- 34 H. Wu, D. Xiao, J. Lu, T. Li, C. Jiao, S. Li, P. Lu and Z. Zhang, Preparation and Properties of Biocomposite Films Based on Poly(vinyl alcohol) Incorporated with Eggshell Powder as a Biological Filler, *J. Polym. Environ.*, 2020, **28**, 2020–2028, DOI: [10.1007/s10924-020-01747-2](https://doi.org/10.1007/s10924-020-01747-2).
- 35 A. A. Oyekanmi, U. S. U. Kumar, H. P. S. Abdul Khalil, N. G. Olaiya, A. A. Amirul, A. A. Rahman, A. Nuryawan, C. K. Abdullah and S. Rizal, Functional properties of antimicrobial neem leaves extract based macroalgae biofilms for potential use as active dry packaging applications, *Polymers*, 2021, **13**, 1664, DOI: [10.3390/polym13101664](https://doi.org/10.3390/polym13101664).
- 36 H. Wu, D. Xiao, J. Lu, T. Li, C. Jiao, S. Li, P. Lu and Z. Zhang, Preparation and Properties of Biocomposite Films Based on Poly(vinyl alcohol) Incorporated with Eggshell Powder as a Biological Filler, *J. Polym. Environ.*, 2020, **28**, 2020–2028, DOI: [10.1007/s10924-020-01747-2](https://doi.org/10.1007/s10924-020-01747-2).
- 37 P. Awasthi, S. C. Singh and R. Kumar, in. *Postharvest Technology of Horticultural Crops*, 2023, DOI: [10.4324/9781032627656](https://doi.org/10.4324/9781032627656).
- 38 L. Vermeiren, F. Devlieghere, M. Van Beest, N. De Kruijf and J. Debevere, Developments in the active packaging of foods, *Trends Food Sci. Technol.*, 1999, **10**, 77–86, DOI: [10.1016/S0924-2244\(99\)00032-1](https://doi.org/10.1016/S0924-2244(99)00032-1).
- 39 J. P. Kerry, M. N. O'Grady and S. A. Hogan, Past, current and potential utilisation of active and intelligent packaging systems for meat and muscle-based products: A review, *Meat Sci.*, 2006, **74**, 113–130, DOI: [10.1016/j.meatsci.2006.04.024](https://doi.org/10.1016/j.meatsci.2006.04.024).
- 40 M. M. Rahman Khan, M. M. H. Rumon and M. Islam, Synthesis, Rheology, Morphology, and Mechanical Properties of Biodegradable PVA-Based Composite Films: A Review on Recent Progress, *Processes*, 2024, **12**, 1–21, DOI: [10.3390/pr12122880](https://doi.org/10.3390/pr12122880).

